Full paper / Mémoire

Charge transfer complexes and cation radical salts of azino-diselenadiazafulvalene

Zdenko Časar [a,b], Ivan Leban [b], Alenka Majcen-le Marechal [c], Lidia Piekara-Sady [a,d], Dominique Lorcy [a,*]

[a] *Sciences Chimiques de Rennes, UMR 6226 CNRS-Université de Rennes 1, Campus de Beaulieu, Bât 10A, 35042 Rennes cedex, France*
[b] *Faculty of Chemistry and Chemical Technology, University of Ljubljana, Aškerčeva 5, 1000 Ljubljana, Slovenia*
[c] *University of Maribor, Smetanova 17, 2000 Maribor, Slovenia*
[d] *Institute of Molecular Physics, Polish Academy of Sciences, Smoluchowskiego 17, 60-179 Poznan, Poland*

Abstract

The synthesis and the redox behaviour of electroactive donor molecules incorporating an azino spacer group between a benzoselenazole core and another heterocyclic moiety, either a benzoselenazole one or a thiazole one, are reported. Neutral complexes were obtained with TCNQ and, for the first time with dithiadiazafulvalene or diselenadiazafulvalene derivatives, cation radical salts by electrocrystallization. Crystal structures data of these complexes are presented and their geometries compared with those deduced from theoretical calculations. ***To cite this article: Z. Časar et al., C. R. Chimie 12 (2009).***
© 2008 Académie des sciences. Published by Elsevier Masson SAS. All rights reserved.

Résumé

La synthèse et les propriétés redox d'une famille de donneur électroactifs incorporant un espaceur azino entre une moitié benzosélénazole et un autre hétérocycle, soit benzosélénazole ou thiazole, sont décrites. Des complexes neutres ont été obtenus en présence de TCNQ et, pour la première fois avec des dérivés de type dithiadiazafulvalène ou disélénadiazafulvalène, des sels d'ions radicaux ont pu être isolés par électrocristallisation. Les données cristallographiques des complexes sont présentées et leurs géométries sont comparées à celles obtenues à partir de calculs théoriques. ***Pour citer cet article : Z. Časar et al., C. R. Chimie 12 (2009).***
© 2008 Académie des sciences. Published by Elsevier Masson SAS. All rights reserved.

1. Introduction

Several electron rich olefins, mainly based on the tetrachalcogenofulvalene framework, have been used as precursors of organic materials [1]. Usually, the

---

* Corresponding author.
  E-mail address: dominique.lorcy@univ-rennes1.fr (D. Lorcy).
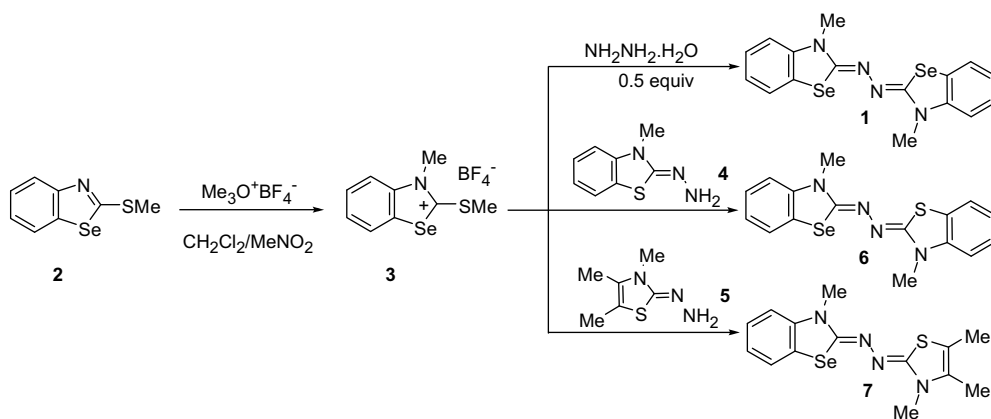
Scheme 1.

donor molecules used in this research area present three well defined oxidation state: neutral, cation radical and dication. Indeed, the physical properties of the organic materials (conductivity, magnetism…) are essentially ascribed to the presence of radical species. Therefore, it is of interest to work with donor molecules which exhibit an easily accessible cation radical state and a thermodynamic stability of this radical. Among the numerous variations realized on the fulvalene skeleton, the insertion of a conjugated spacer group such as an azino one between the two heterocyclic cores gave rise to an interesting family of compounds known as heterocyclic azines [2]. Hünig et al. developed this strategy some years ago and showed that these derivatives present two mono-electronic oxidation waves with excellent reversibility [3]. Additionally, the presence of an azino spacer group increases the window potential stability of the cation radical species. Within these azino derivatives, Hünig et al., showed that the three oxidation levels of this system could be isolated, but except one further work on conductivity measurements, no other studies were

performed on these donors such as structural or EPR [4]. In an earlier study we examined the potential of azino-dithiadiazafulvalenes as precursors of charge transfer complexes in the presence of TCNQ [5]. Herein we decided to investigate the ability of the azinodibenzodiselenadiazafulvalene **1** as precursor of charge transfer salts. Furthermore, we also prepared unsymmetrical donors where we replaced one benzoselenazole moiety with thiazole cores in order to modulate the redox properties of these donor systems. In this article we will present also the X-ray structure of the complexes obtained with TCNQ oxidation or by using the electrocrystallisation technique as well as molecular geometry optimizations performed by DFT calculations in order to rationalize the geometries' evolutions and electrochemical properties.
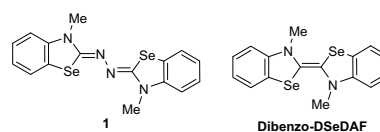
2. Results and discussion

2.1. Synthesis and electrochemical studies

In order to prepare the symmetrical azino-DSeDAF **1**, we followed Hünig's strategy which consists of the reaction of quaternary heterocyclic salts with a half equivalent of hydrazine in a basic medium (Scheme 1) [3]. First, we prepared 3-methyl-2-methylthio-benzoselenazolium salt **3** from 2-methylthio-benzoselenazole **2** [6] with a new one-step approach in 91% yield. The synthesis of N,N′-bis(benzo-3H-selenazol-2-ylidene)-hydrazine (azino-DSeDAF) **1** was performed by

Table 1
Redox properties of azino-dichalcogenodiazafulvalenes n-Bu$_4$NPF$_6$, 100 mV/s.

Donor	E_1	E_2	$E_2 - E_1$ mV (K)
1[a]	0.53	1.07	540 (1.42×10^9)
1[b]	0.56	1.01	450 (4.23×10^7)
5[b]	0.54	1.00	460 (6.26×10^7)
6[b]	0.29	0.81	520 (6.5×10^8)
Dibenzo-DSeDAF [6]	−0.07[c]	0.09[c]	160 (5.1×10^2)
Dibenzo-TSeF [12]	0.78	1.17	390 (4.07×10^6)

[a] CH$_2$Cl$_2$.
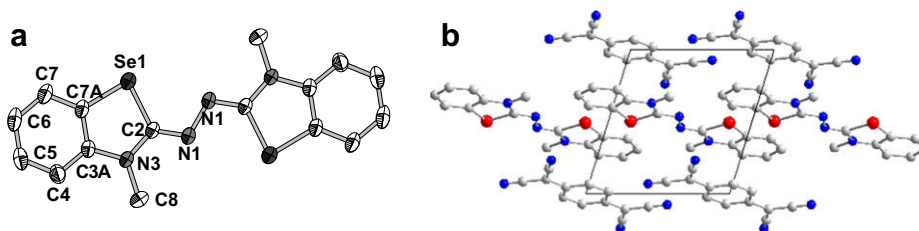[b] CH$_3$CN.
[c] Oxidation peak potential.

Fig. 1. (a) View of the molecular structure of **1** in (**1**)(TCNQ) showing the atom labelling. Hydrogen atoms are omitted for clarity (50% probability ellipsoids). (b) View of the unit cell along *ab* plane.

using salt **3** in the presence of NEt$_3$ and half an equivalent of hydrazine hydrate, affording azino-DSeDAF **1** in 55% yield. For the synthesis of unsymmetrical azino donors, containing one selenazole and one thiazole cores, we first prepared the appropriate heterocyclic hydrazones **4** and **5** [5] which are consequently coupled with selenazolium salt **3** in basic medium as depicted in Scheme 1. Indeed, the reaction between selenazolium salt **3** and 3-methyl-3*H*-benzothiazol-2-one hydrazone **4** [7] in MeCN/EtOH in the presence of NEt$_3$ afforded azinodibenzoselenathiadiazafulvalene (azino-dibenzo-SeTDAF) **6** in 70% yield. Treatment of 3,4,5-trimethyl-3*H*-thiazol-2-one hydrazone **5** with salt **3** under the same conditions resulted in the formation of azino-benzotetramethylselenathiadiazafulvalene (azino-benzoTMSeTAF) **7** which was isolated in 83% yield.
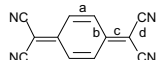
Electrochemical investigations were performed using tetrabutylamonium hexafluorophosphate as supporting electrolyte. In all cases, cyclic voltammetry revealed two monoelectronic reversible oxidation waves with a difference between the two oxidation potentials ΔE larger than 450 mV ($\Delta E = E_2 - E_1$, $K \geq 4.23 \times 10^7$ Table 1). This indicates a very high thermodynamic stability of the cation radical species induced by the azino spacer group as for example the parent dibenzo-DSeDAF exhibits a smaller ΔE ($K = 5.1 \times 10^2$, $K = [D^{+\bullet}]^2/[D][D^{2+}]$). Comparison of the redox potentials

between dibenzo-DSeDAF ($E_{pa}^1 = -0.07$ V and $E_{pa}^2 = 0.09$ V vs SCE in CH$_2$Cl$_2$) [6a] and azinodibenzo-DSeDAF **1** indicates that the presence of the azino spacer group induces an important anodic shift of the two oxidation potentials. Therefore, **1** is stable under atmospheric conditions while dibenzo-DSeDaF oxidizes readily upon air exposure. Furthermore, substitution of one selenium atom in the azino-dibenzo-DSeDAF **1** with sulfur one does not significantly modify the donor ability, since for **5** E_1 is only 20 mV lower than for **1**. Similarly, the effect on ΔE is negligible since a difference of 10 mV is observed (Table 1). The most pronounced effect on E_1 was observed when one benzoselenazole core in **1** was replaced with the 3,4,5,-trimethyl-thiazole one. Indeed, azino-benzoTMSeTDAF **6** has the best electron donating ability in the synthesized azino series ($E_1 = 0.29$ V vs SCE). This unambiguously demonstrates that benzo-fusion decreases the donor ability.

2.2. TCNQ complexes

In order to form charge transfer salts with these azino derivatives, we tried both chemical and electrochemical pathways. For the chemical approach, we simply mixed a hot solution of the donor in CH$_2$Cl$_2$ with a hot solution of TCNQ in CH$_3$CN. Treatment of azine **1**, **6** and **7** solutions with TCNQ resulted in the formation of poorly soluble azine–TCNQ complexes which precipitated from the medium as microcrystalline materials in high yields for **1** and **6** (82% and 84% yields, respectively) while in low yield for **7** (19%). Elemental analysis shows that 1:1 complexes were formed in all three cases. FT-IR spectra revealed that all three isolated complexes exhibit a single sharp ν_{CN} band at 2218 cm^{-1} for (**1**)(TCNQ) and (**6**)(TCNQ) and at 2212 cm^{-1} for (**7**)(TCNQ). Based on the nitrile stretching absorption band, it is possible to infer the degree of charge transfer in TCNQ complexes [8]. The

Table 2
Averaged distances (*a*–*d*) in TCNQ.

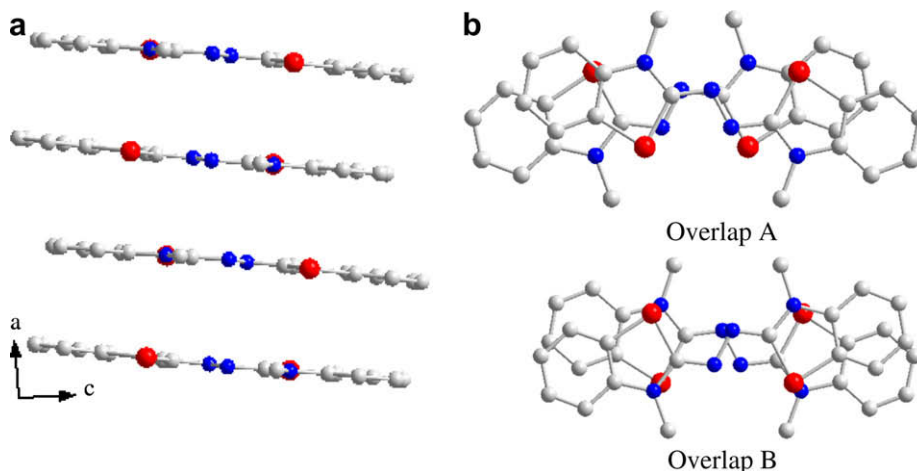|	Neutral TCNQ [10]	(**1**)(TCNQ)
a	1.346(3)	1.338(3)
b	1.448(4)	1.441(3)
c	1.374(3)	1.374(3)
d	1.441(3)	1.433(4)

Fig. 2. Crystal structure of complex (**1**)(PF$_6$). (a) Projection onto the *ac* plane showing the segregated stack of donors. (b) Showing the overlap modes between two neighbouring donors **1**.

value obtained for the three complexes are close to the one observed for neutral TCNQ ν_{CN} at 2224 cm^{-1} which indicates that these materials are neutral charge transfer complexes [9]. This was confirmed by EPR experiments as no EPR signal was observed from room temperature to liquid helium temperature. This result is consistent with the presence of neutral complexes.

Crystals were obtained for complex (**1**)(TCNQ) and the crystal structure determination confirms a stoichiometry of one donor **1** for one TCNQ. It crystallizes in the triclinic system, space group *P*-1 with both the donor and TCNQ molecules located on an inversion center. Within this complex, donor molecules form alternated stacks with TCNQ. The plane of the donor is not fully parallel to the plane of the acceptor but forms an angle of 2.9(3)° with an interplanar separation of

3.47 Å (Fig. 1). This organization is reminiscent of what we previously observed with (azino-dithiadiaza-fulvalenes)(TCNQ) complexes [5]. Analysis of the bond lengths in the TCNQ skeleton shows that they are essentially similar to those reported for the neutral TCNQ [10] (see Table 2), confirming that the complex (**1**)(TCNQ) is neutral. Actually, the potential difference between the reduction potential of TCNQ (0.18 V) and the oxidation potential of **1** (0.56 V) is too large for allowing any redox reaction. Thus, in this case, we are dealing with co-crystallization of the two components rather than with an electron transfer process.

2.3. Electrocrystallization

Then, we focused our attention on the electrochemical pathway which consists in using the electrocrystallization technique, an invaluable tool for the elaboration of ordered electroactive molecular charge transfer salts [11]. Deep blue needles grew on the anode within a couple of days from donor **1** by using *n*-Bu$_4$NPF$_6$ as the supporting electrolyte in CH$_2$Cl$_2$. The structure of the salt was determined by X-ray diffraction studies and revealed a stoichiometry of one donor for one PF$_6^-$ anion, the first example of isolated cation radical salts in these series.

The salt (**1**)(PF$_6$) crystallizes in the monoclinic system, space group *C*2/*c* with one donor molecule and one PF$_6^-$ anion both in general position in the unit cell, hence a 1:1 stoichiometry. Within this salt, the oxidized donor molecules form segregated stacks (Fig. 2a). Two types of overlap are observed as depicted in Fig. 2b. Mean plane distances between

Table 3
Averaged bond length of donor **1** in (**1**)(TCNQ) and in (**1**)(PF$_6$) and B3LYP/LANL2DZ optimized bond lengths for **1** and **1**$^{+\bullet}$ in Å.

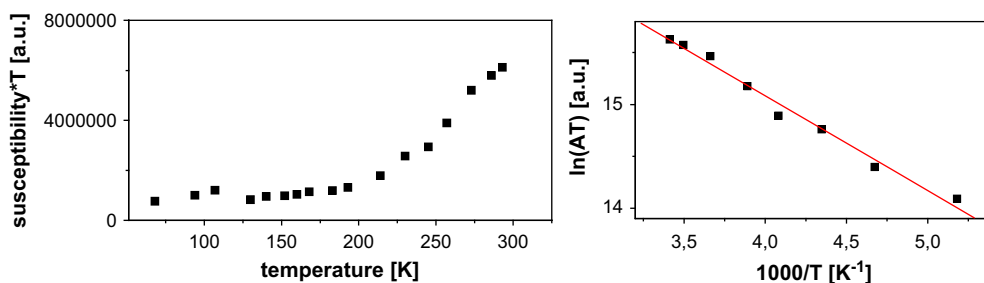|	In complex (**1**)(TCNQ)	In complex (**1**)(PF$_6$)	**1** (DFT)	**1**$^{+\bullet}$(DFT)
a	1.414(4)	1.354(6)	1.414	1.361
b	1.286(3)	1.312(7)	1.301	1.339
		1.322(7)		
c	1.366(3)	1.357(6)	1.392	1.369
		1.343(6)		
d	1.898(2)	1.874(4)	1.967	1.937
		1.864(4)		
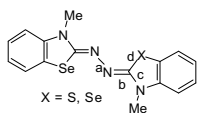
Fig. 3. (Left) Temperature dependence of $\chi_s T$ derived from the EPR of $(\mathbf{1}^{\bullet})(PF_6)$. (Right) Linear fit to $\ln(\chi_s T) = -(\Delta/k_B)/T + \ln C$ above 200 K.

donor molecules within one stack are, respectively, of 3.37 Å and 3.64 Å for overlap A and B. Furthermore, the donor core in its cation radical state is planar, as the structure of the donor $\mathbf{1}$ under neutral state in $(\mathbf{1})(TCNQ)$. On the other hand, modification of the bond lengths of the donor skeleton is observed in the oxidized donor core essentially on the central spacer group. In the oxidized species the double bond $C=N$ is lengthened while the central $N-N$ bond is shortened when compared with the neutral molecule (Table 3). The $C-Se$ and $C-N$ cyclic bonds are also shortened in the oxidized species compared with the neutral one.

The EPR study was carried out on a polycrystalline sample of $(\mathbf{1})PF_6$. A single Lorentzian shaped line was observed at $g = 2.007$ with a linewidth of 40 G at room temperature. Since PF_6^- is diamagnetic, this signal is due to the radical cation of $\mathbf{1}^{\bullet}$. The temperature dependence of the signal was studied using the well-known approximation that spin susceptibility is proportional to the product: $A(\Delta B_{pp})^2$, where A is the line amplitude and ΔB_{pp} – peak-to-peak linewidth. The result is displayed in Fig. 3 as $\chi_s T$. From 70 K to $\sim$200 K spin susceptibility, within the experimental error, is constant, i.e. the Curie law is obeyed. Above 200 K there is a thermally activated slow increase in susceptibility which is a sign of a singlet–triplet behaviour associated with the dimerization of cations observed in the X-ray crystal structure (Fig. 2). Similarly, the linewidth decreases with lowering temperature from 40 G at room temperature to $\sim$20 G at 200 K. Further decrease in temperature does not change the linewidth significantly (Fig. 4). Both $\chi_s T$ and ΔB_{pp} temperature evolution confirm a thermally activated susceptibility above 200 K. One can estimate singlet–triplet energy gap Δ/k_B of ca. 900 K (630 cm^{-1}) (Fig. 3, right).

2.4. Molecular geometry optimization

DFT calculations [B3LYP/LANL2DZ] were performed on the azinodibenzo-DSeDAF $\mathbf{1}$ and the

oxidized species $\mathbf{1}^{+\bullet}$, and, for comparison purpose, on the dibenzo-tetraselenafulvalene (TSeF) and the dibenzo-DSeDAF in order to determine the highest occupied molecular orbitals (HOMO) energies as well as their electron density contours. As shown in Fig. 5, the energy of the HOMO of $\mathbf{1}$ ($E = -4.89$ eV) is located in between those of dibenzo-TSeF ($E = -5.00$ eV) and dibenzo-DSeDAF ($E = -4.42$ eV), but closer in energy to the TSeF system. This evolution of the HOMOs was anticipated from their redox potentials determined by cyclic voltammetry, as for instance the redox potentials of the dibenzo-TSeF, $E_1 = 0.78$ V and $E_2 = 1.17$ V vs SCE in CH_2Cl_2, are closer to the redox potential of $\mathbf{1}$ compared with the dibenzo-DSeDAF [12]. These energies of the HOMO also explain the higher oxidation potentials observed for the $\mathbf{1}$ derivatives compared with DSeDAF. The topology of the HOMO for the selenazole rings in $\mathbf{1}$ and the dibenzo-DSeDAF is similar showing antibonding interactions between the selenium or the nitrogen and the carbon atoms. Concerning the conjugated spacer group in $\mathbf{1}$, bonding interactions are observed between the nitrogen and the carbon atoms while an antibonding interaction connect the two nitrogen atoms inducing a destabilization of the HOMO and generating a higher oxidation potential
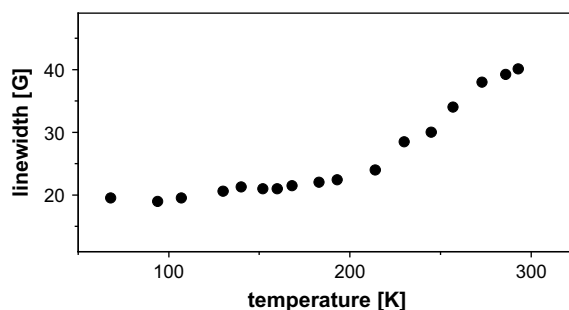

Fig. 4. Temperature dependence of the EPR peak-to-peak linewidh of $(\mathbf{1}^{\bullet})(PF_6)$.

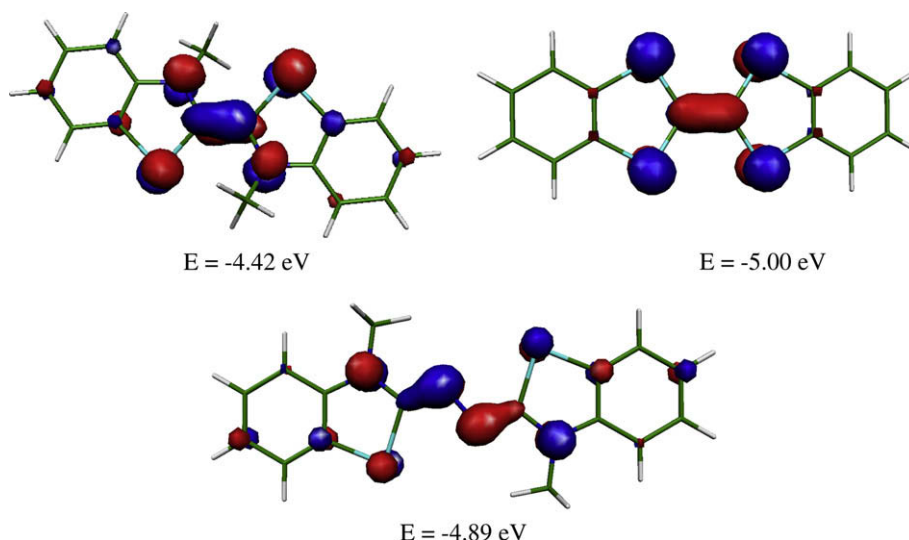E = -4.42 eV   E = -5.00 eV

E = -4.89 eV

Fig. 5. Molecular orbital surfaces and HOMO levels of dibenzo-DSeDAF (top left), dibenzo-TSeF (top right) and azinodibenzo-DSeDAF neutral (bottom).

Table 4
Crystal data and structure refinement parameters for (**1**)(TCNQ) and (**1**)(PF$_6$).

Structure parameter	(**1**)(TCNQ)	(**1**)(PF$_6$)
Empirical formula	$C_{16}H_{14}N_4Se_2$, $C_{12}H_4N_4$	$C_{16}H_{14}N_4Se_2$, PF_6
Molecular weight	624.42	565.20
Crystal system	Triclinic	Monoclinic
Space group	P-1	$C2/c$
a (Å)	8.5649(2)	7.1183(5)
b (Å)	9.1230(2)	20.4029(11)
c (Å)	9.8916(2)	28.750(2)
α (°)	68.4690(10)	90
β (°)	72.1990(10)	91.610(8)
γ (°)	67.8490(10)	90
V (Å^3)	653.23(3)	4173.8(5)
T (K)	293(2)	293(2)
Z	1	8
F000	310	2200
D_{calc} (g/cm^3)	1.587	1.799
μ (mm^{-1})	2.864	3.682
Total number of measured intensities	14,983	13,528
Abs corr	Multiscan	Multiscan
Number of unique data	2961(0.0285)	3912(0.0771)
Observed reflections ($I > 2\sigma(I)$)	2677	2267
Number of refined variables (n)	180	298
R_1, wR_2	0.0356, 0.0956	0.0419, 0.0912
R_1, wR_2 (all data)	0.0309, 0.0905	0.0874, 0.1029
GoF	1.054	0.876

than for dibenzo-DSeDAF. It is interesting to note the small coefficient at the C4 carbon atom of the selenazole rings on both the DSeDAF and the azino derivative. This small coefficient on the carbon located alpha to the NMe group has already been noticed on the thiazole ring of sulfur analogues, DTDAF [13]. Optimized bond lengths calculated for azinodibenzo-DSeDAF **1** and the oxidized species **1**$^{+\bullet}$ are reported in Table 3. If we compare the optimized geometry and bond lengths calculated for **1** with the X-ray data in (**1**)(TCNQ), we can observe that there is a good agreement for the neutral state of the donor in the complex, (**1**)(TCNQ). Moreover the optimized bond length calculated for **1**$^{+\bullet}$ shows that oxidation affects essentially the bonds in which the electron density in the HOMO is concentrated, in agreement with the experimental evidence (**1**)(PF$_6$).

3. Conclusion

In this study, a series of bis(benzoselenazolydene)-hydrazine have been synthesized and their redox properties have been electrochemically determined. A first example of a cation radical salt of such azino derivatives has been electrochemically crystallized and structurally characterized. This is in sharp contrast with the recurrent decomposition observed with the "classical" DSeDAF or dithiadiazafulvalene (DTDAF) derivatives. Future work is in progress for exploring the potentialities of these azino donors upon electro-crystallization experiments.

4. Experimental

4.1. General

^{1}H NMR spectra were recorded at 300 MHz and ^{13}C NMR spectra at 75 MHz with tetramethylsilane as internal reference. Mass spectra were carried out at Centre de Mesures Physiques de l'Ouest, Rennes. Melting points were measured using a Kofler hot stage apparatus and are uncorrected. Elemental analysis results were obtained from the Laboratoire Central de Microanalyse du CNRS (Lyon). Cyclic voltammetry was carried out on a 10^{-3} M solution of metal complex derivative in CH_2Cl_2 containing 0.1 M n-Bu$_4$NPF$_6$ as supporting electrolyte. Voltammograms were recorded at 0.1 V s^{-1} on a platinum disk electrode (1 mm^2). Potentials were measured vs Saturated Calomel Electrode (SCE). The EPR measurements were performed on Bruker ESP-300E X-band spectrometer equipped with a helium Oxford kriostat using liquid nitrogen as cooling agent.

4.2. Synthesis and characterization

4.2.1. 3-Methyl-2-methylthio-benzoselenazolium tetrafluoroborate (3)

To a stirred solution of 2-methylthio-benzoselenazole **2** (2.25 g, 9.86 mmol) in CH_2Cl_2 (10 mL) was added trimethyloxonium tetrafluoroborate (1.46 g, 9.86 mmol) in CH_2Cl_2/MeNO$_2$ (5 mL/9 mL). The reaction mixture was stirred at room temperature for 52 h. The solvent was evaporated and CH_2Cl_2 (10 mL) was added to the residue. The mixture was treated with Et$_2$O (35 mL). The precipitate was filtered washed with Et$_2$O and dried to give 3-methyl-2-methylthio-benzoselenazolium tetrafluoroborate **3** as white powder in 91% yield (2.97 g) as a white powder, mp 187 °C. ^{1}H NMR (CD$_3$CN): δ 8.13−8.00 (1H, dd, $J_1 = 8.1$ Hz, $J_2 = 1.0$ Hz), 7.85−7.72 (1H, dd, $J_1 = 8.3$ Hz, $J_2 = 0.8$ Hz), 7.70−7.58 (1H, td, $J_1 = 7.3$ Hz, $J_2 = 1.3$ Hz), 7.56−7.42 (1H, td, $J_1 = 7.3$ Hz, $J_2 = 1.3$ Hz), 3.87 (3H, s), 2.91 (3H, s). ^{13}C NMR (CD$_3$CN): δ 189.4, 143.8, 129.6, 128.8, 126.9, 125.9, 116.6, 37.5, 19.5. Anal. Calcd for C$_9$H$_{10}$NSSeBF$_4$: C, 32.76; H, 3.05; N, 4.24. Found: C, 32.50; H, 2.94; N, 4.05.

4.2.2. Azino-dibenzoDSeTDAF (1)

To a stirred suspension of 3-methyl-2-methylthio-benzoselenazolium tetrafluoroborate **2** (1.20 g, 3.64 mmol) in absolute EtOH (8 mL) were added NEt$_3$ (0.74 g, 7.27 mmol) in absolute EtOH (2 mL) and

H$_2$N−NH$_2$·H$_2$O (88.2 μL, 1.82 mmol). The mixture was stirred at room temperature for 40 min. The precipitated product was filtered off and dried to give pale yellow powder. The crude product was suspended in 100 mL of water and suspension was stirred at room temperature for 30 min. Undissolved white solid was filtered and dried on air at room temperature to give white powder, which was recrystallized from petroleum ether/CH_2Cl_2 to furnish azino-DSeDAF **1** in 55% yield (0.42 g) as white powder, R_f (CH$_2$Cl$_2$) = 0.72, mp 273 °C (lit. [2] 270−272 °C). ^{1}H NMR (acetone-d_6): δ 7.66−7.57 (2H, dd, $J_1 = 7.6$ Hz, $J_2 = 1.0$ Hz), 7.39−7.27 (2H, td, $J_1 = 7.8$ Hz, $J_2 = 1.3$ Hz), 7.17−7.09 (2H, dd, $J_1 = 8.1$ Hz, $J_2 = 1.0$ Hz), 7.06−7.96 (2H, td, $J_1 = 7.6$ Hz, $J_2 = 1.0$ Hz), 3.58 (6H, s). ^{13}C NMR (CDCl$_3$): δ 159.6, 143.8, 126.7, 126.0, 122.8, 121.3, 110.0, 31.5. MS m/z (relative intensity) 422 (M$^+$, 100), 374 (47), 225 (10), 197 (24), 184 (37). HRMS: calcd for C$_{16}$H$_{14}$N$_4$Se$_2$: 421.9549. Found: 421.9565. Anal. Calcd for C$_{16}$H$_{14}$N$_4$Se$_2$: C, 45.73; H, 3.36; N, 13.33. Found: C, 45.82; H, 3.53; N, 13.37.

4.2.3. Azino-dibenzoSeTDAF (6)

To a stirred suspension of 3-methyl-3H-benzo-thiazol-2-one hydrazone **4** (0.18 g, 1.00 mmol) in absolute EtOH (4 mL) were added NEt$_3$ (0.10 g, 1.00 mmol) in absolute EtOH (2 mL) and 3-methyl-2-methylthio-benzoselenazolium tetrafluoroborate **3** (0.33 g, 1.00 mmol) in MeCN (6 mL). The mixture was stirred under nitrogen at room temperature for 45 min. The precipitated product was filtered off, washed with absolute EtOH (10 mL) and dried to give white crystalline powder, which was recrystallized from petrol ether/CH_2Cl_2 to furnish azine **6** in 70% yield (0.26 g), white powder, R_f (CH$_2$Cl$_2$) = 0.74, mp 268 °C. ^{1}H NMR (DMSO-d_6): δ 7.69−7.62 (1H, dd, $J_1 = 7.8$ Hz, $J_2 = 1.3$ Hz), 7.59−7.52 (1H, dd, $J_1 = 7.6$ Hz, $J_2 = 0.8$ Hz), 7.37−7.25 (2H, m), 7.22−7.11 (2H, td, $J_1 = 8.1$ Hz, $J_2 = 1.0$ Hz), 7.09−6.94 (2H, m), 3.52 (3H, s), 3.49 (3H, s). ^{13}C NMR (CDCl$_3$): δ 159.6, 159.3, 143.9, 142.1, 126.7, 126.4, 126.0, 124.8, 122.8, 122.4, 121.2, 121.1, 109.9, 108.7, 31.9, 30.9. MS m/z (relative intensity) 374 (M$^+$, 100), 326 (25), 212 (5), 197 (10), 164 (18), 149 (22). HRMS: calcd for C$_{16}$H$_{14}$N$_4$SSe: 374.0104. Found: 374.0116. Anal. Calcd for C$_{16}$H$_{14}$N$_4$SSe: C, 51.47; H, 3.78; N, 15.00. Found: C, 51.76; H, 3.83; N, 15.23.

4.2.4. Azino-benzoTMSeTDAF (7)

To a stirred solution of 3,4,5-trimethyl-3H-thiazol-2-one hydrazone **5** (0.26 g, 1.67 mmol) in absolute

EtOH/MeCN = 1:1 (16 mL) was added 3-methyl-2-methylthio-benzoselenazolium tetrafluoroborate **3** (0.55 g, 1.67 mmol) and NEt$_3$ (0.17 g, 1.67 mmol). The mixture was stirred under nitrogen at room temperature for 60 min. The precipitated product was filtered off, washed with absolute EtOH (25 mL) and dried to give green powder, which was recrystallized from petrol ether/CH$_2$Cl$_2$ to furnish azine **7** in 83% yield (0.49 g), light green cubes, R_f (CH$_2$Cl$_2$) = 0.45, mp 249 °C. ^{1}H NMR (CDCl$_3$): δ 7.50–7.42 (1H, dd, J_1 = 7.6 Hz, J_2 = 1.3 Hz), 7.28–7.21 (1H, dd, J_1 = 7.8 Hz, J_2 = 1.3 Hz), 6.99–6.86 (2H, m), 3.56 (3H, s), 3.35 (3H, s), 2.09 (3H, s), 2.04 (3H, s). ^{13}C NMR (pyridine-d_5): δ 164.2, 158.6, 146.4, 132.1, 129.1, 128.4, 125.0, 123.2, 112.2, 106.5, 33.8, 33.5, 14.2, 13.1. MS m/z (relative intensity) 352 (M$^+$, 100), 304 (15), 197 (5), 184 (6), 176 (8), 156 (7), 141 (12), 127 (12). HRMS: calcd for C$_{14}$H$_{16}$N$_4$SSe: 352.0261. Found: 352.0275. Anal. Calcd for C$_{14}$H$_{16}$N$_4$SSe: C, 47.86; H, 4.59; N, 15.95. Found: C, 48.06; H, 4.56; N, 16.19.

4.2.5. TCNQ complexes

To a solution of azino donor (0.2 mmol) in CH$_2$Cl$_2$ (9 mL) was added a hot solution of TCNQ (0.2 mmol) in MeCN (8 mL). The mixture was left to stand at room temperature for 2–3 days. The precipitate was filtered and dried to give the azine·TCNQ complexes.

(**1**)(TCNQ): 82% yield, brown-red needles, mp 283 °C (dec). IR (KBr): ν_{CN}/cm^{-1} 2218. Anal. Calcd for C$_{28}$H$_{18}$N$_8$Se$_2$: C, 53.86; H, 2.91; N, 17.95. Found: C, 54.15; H, 2.83; N, 17.68.

(**6**)(TCNQ): 84% yield, brown-red needles, mp 279 °C (dec). IR (KBr): ν_{CN}/cm^{-1} 2218. Anal. Calcd for C$_{28}$H$_{18}$N$_8$SSe: C, 58.23; H, 3.14; N, 19.40. Found: C, 58.48; H, 2.93; N, 19.17.

(**7**)(TCNQ): 19% yield, violet-red microcrystalline solid, mp 250 °C (dec). IR (KBr): ν_{CN}/cm^{-1} 2212. Anal. Calcd for C$_{26}$H$_{20}$N$_8$SSe: C, 56.21; H, 3.63; N, 20.17. Found: C, 56.57; H, 3.39; N, 20.21.

4.3. Electrocrystallization

Into a 30 mL H-shaped glass cell with a fine frit dividing the anodic and cathodic compartments equipped with platinum wire electrodes was placed a solution of tetrabutylammonium hexafluorophosphate (∼3 g) in CH$_2$Cl$_2$ (30 mL). The azine donor **1** (10 mg) was added into the anode compartment. The solution was electrolyzed under a constant current of 2 μA at room temperature. Blue crystals of radical cation salts gradually grew on the anode electrode within several days. The crystals were collected by filtration, washed with cold CH$_2$Cl$_2$ and dried. The obtained crystals were utilized for X-ray crystallographic analyses.

4.4. Crystallography

Single-crystal diffraction data were collected on a Nonius KappaCCD diffractometer from the University of Ljubljana for complex (**1**)(TCNQ) and on a Stoe IPDS diffraction system from the University of Angers for compound (**1**)(PF$_6$). Details of the crystallographic are given in Table 4.

5. Supplementary material

Crystallographic data for structural analysis have been deposited with the Cambridge Crystallographic Data Centre, CCDC nos. 695874–695875 for compound (**1**)(TCNQ) and (**1**)(PF$_6$), respectively. Copies of this information may be obtained free of charge from The Director, CCDC, 12 Union road, Cambridge CB2 1EZ, UK (fax: +44 1223 336033; e-mail: deposit@ccdc.cam.ac.uk or http://www.ccdc.cam.ac.uk).

References

[1] Special issue on "Molecular conductors" P. Batail, Chem. Rev. 104 (2004) 4887.
[2] S. Hünig, G. Kießlich, F. Linhart, H. Schlaf, Justus Liebigs Ann. Chem. 752 (1971) 182.
[3] S. Hünig, G. Kießlich, F. Linhart, H. Schlaf, Justus Liebigs Ann. Chem. 752 (1971) 196.
[4] W.A. Barlow, G.R. Davies, E.P. Goodings, R.L. Hand, G. Owen, M. Rhodes, Mol. Cryst. Liq. Cryst. 33 (1976) 123.
[5] D. Guérin, D. Lorcy, R. Carlier, S. Los, L. Piekara-Sady, J. Solid State Chem. 168 (2002) 590.
[6] (a) Z. Časar, P. Bénard-Rocherullé, A. Majcen-Le Maréchal, D. Lorcy, Chem. Commun. (2001) 1336;
(b) Z. Časar, I. Leban, A. Majcen-Le Maréchal, D. Lorcy, J. Chem. Soc., Perkin Trans. 1 (2002) 1568.
[7] S. Hünig, H. Balli, Justus Liebigs Ann. Chem. 609 (1957) 160.

[8] J.S. Chappel, A.N. Bloch, W.A. Bryden, M. Maxfield, T.O. Poehler, D.O. Cowan, J. Am. Chem. Soc. 103 (1981) 2442.

[9] F.H. Herbstein, in: J.D. Dunitz, J.A. Ibers (Eds.), Perspectives in Structural Chemistry, vol. 4, Wiley, New York, 1971, p. 166.

[10] R.E. Long, R.A. Sparks, K.N. Trueblood, Acta Crystallogr. 18 (1965) 932.

[11] P. Batail, M. Fourmigué, K. Boubekeur, J.-C. Gabriel, Chem. Mater. 10 (1998) 3005.

[12] K. Lerstrup, D. Talham, A. Bloch, T. Poehler, D. Cowan, J. Chem. Soc., Chem. Commun. (1982) 332.

[13] S. Eid, M. Guerro, T. Roisnel, D. Lorcy, Org. Lett. 8 (2006) 2377.